Novel combination of hydrophilic/hydrophobic surface for large wettability difference and its application to liquid manipulation†

Taizo Kobayashi,[a] Kazunori Shimizu,[ab] Yoshihiro Kaizuma[c] and Satoshi Konishi*[d]

Received 10th September 2010, Accepted 29th October 2010
DOI: 10.1039/c0lc00394h

This paper reports a novel combination of hydrophilic/hydrophobic materials for the evolution of liquid manipulation. Droplet generation based on a hydrophilic/hydrophobic mechanism is a promising method for highly accurate liquid manipulations. Although several droplet manipulation devices utilizing hydrophilic/hydrophobic patterns have been reported, it has been difficult to split fluid into droplets solely through hydrophilic/hydrophobic patterns in a microchannel. In this study, a material combination for fabricating hydrophilic/hydrophobic patterns was investigated and their wettability difference was enhanced for droplet generation. To improve hydrophilicity, we attempted to increase the surface area of silicon oxide through pulsed plasma chemical vapor deposition (PPCVD). To improve hydrophobicity, the damage to the hydrophobic patterns in the fabrication process was reduced. We successfully enhanced the difference in contact angles from 54.3° to 86.6° by combining the developed hydrophilic material and hydrophobic material. The developed material combination could successfully split fluid into a quantitative droplet of 14.1 nL in a microfluidic chip. Because the developed hydrophilic/hydrophobic combination enables the formation of a droplet with desirable shape in microchannels, the developed hydrophilic/hydrophobic combination is a promising component for lab-on-a-chip applications.

Introduction

Surface wettability control has become essential in various microfluidic applications, such as quantitative liquid metering and microcapillaries. Droplet generation based on the hydrophilic/hydrophobic mechanism is a promising method for highly accurate liquid metering.[1] For example, Handique *et al.* have reported an on-chip minute liquid metering device utilizing a combination of hydrophobic liquid stopper and air pressure.[2,3] A droplet extraction device that is a combination of a deformable wall and hydrophobic patterns was reported in our previous study.[4] It is important for on-chip liquid metering to split liquid accurately. A functional surface consisting of a hydrophilic material and a hydrophobic material is a promising component for liquid metering applications. Although it has been suggested that hydrophilic islands surrounded by hydrophobic regions will make it much easier to carry out droplet generation, it was difficult to carry out droplet generation in a microchannel employing only the wettability difference. Droplet generation based on the hydrophilic/hydrophobic mechanism requires a large wettability difference. In this study, we attempt to enhance both hydrophilicity and hydrophobicity to realize a novel combination of hydrophilic/hydrophobic materials.

Recently, superhydrophilic and superhydrophobic surfaces utilizing nanometre-scale biomimetic surfaces or photocatalysts have been reported, for example, a lotus-like surface,[5] a desert beetle-like surface,[6] a fractal structured surface[7] and a micropatterned photocatalytic material.[8] Previously, the co-author found that the pulsed plasma chemical vapor deposition (PPCVD) formed a nanostructured silicon oxide with large surface area.[9]

In addition, our group has reported surface wettability control of a patterned perfluoropolymer by reducing the damage in the fabrication process.[10] It is possible to pattern the perfluoropolymer without reducing the hydrophobicity in comparison to the as-deposited perfluoropolymer. Our strategy involves combining nanometre-scale surface morphology with the hydrophilic/hydrophobic patterning technique. Silicon oxide with a rough surface is combined with the reported perfluoropolymer patterns. The influence of fabrication parameters on the wettability difference and droplet generation accuracy is investigated.

On the basis of the developed hydrophilic/hydrophobic patterns, we propose dome-shaped droplet generation and suspended-shape droplet generation technologies. A suspended-shape droplet refers to a microsized liquid pillar in which the top and bottom are attached to the ceiling and the bottom of a flow channel. Because the volume of a suspended-shape droplet can be calculated by multiplying the exposed areas of hydrophilic islands and the channel height, it is suggested that droplet technology is suitable for on-chip quantitative titration. The droplet handling method based on centrifugal force is also demonstrated.

[a]*Ritsumeikan Global Innovation Research Organization, Ritsumeikan University, 1-1-1, Noji Higashi, Kusatsu, Shiga, Japan*
[b]*Graduate School of Pharmaceutical Sciences, Kyoto University, 46-29, Shimo-Adachi-Cho, Yoshida, Sakyoku, Kyoto, Japan*
[c]*Shinko Seiki Co., Ltd., 30, Miyake-Cho, Moriyama, Shiga, Japan*
[d]*Department of Micro System Technology, Ritsumeikan University, 1-1-1, Noji Higashi, Kusatsu, Shiga, Japan. E-mail: konishi@se.ritsumei.ac.jp*
† Electronic supplementary information (ESI) available: Movies S1–S3. See DOI: 10.1039/c0lc00394h

Surface wettability control of hydrophilic/hydrophobic patterns

The proposed material combination enables the generation of quantitative droplets in exposed hydrophilic regions, as shown in Fig. 1(a). The conceptual image of the proposed surface integrated into the microfluidic device is shown in Fig. 1(b).

Strategy for enhancement of wettability difference

Our strategy for enhancement of wettability difference is illustrated in Fig. 2. Superhydrophilicity can be obtained by increasing the surface area of silicon oxide (SiO_x) as shown in the upper-left panel of Fig. 2. It is well known that a large surface area reduces the contact angle of a hydrophilic surface, in accordance with Wenzel's equation:[11,12]

$$\cos \theta^* = r \times \cos \theta$$

θ^*: contact angle on an ideal surface, θ: apparent contact angle on a solid surface, and r: surface roughness ratio given by surface area/projection area.

The strategy to enhance the hydrophobic patterns is shown in the upper-right panel of Fig. 2. The mask material and the additional postannealing process were optimized to enhance the hydrophobicity of perfluoropolymer patterns.[10] The lower panel of Fig. 2 shows a schematic view of the combination of roughness-controlled SiO_x and damage-reduced CYTOP® patterns for a large wettability difference.

Deposition of roughness-controlled silicon oxide

SiO_x with a large surface area can be obtained by the PPCVD method. A co-author has previously reported details of PPCVD and the setup.[9] The surface of SiO_x becomes rougher through the application of a pulsed radio frequency (RF) power in a relatively high-pressure environment in the PCVD process. The sequence of the pulse patterns of RF power and supplied gases is presented in Table 1. Ingredient gases contained $Si(CH_3)_4$, Ar and O_2. The width and interval of RF pulses were set at 220 ms and 2.2 ms, respectively. Mean RF power was adjusted to 200 W. The pulsed gas of $Si(CH_3)_4$ was supplied at a duty ratio of 10%. Ar and O_2 were supplied continuously. In conventional continuous PCVD (CPCVD), the RF power was supplied continuously and was adjusted to 200 W. Samples A and B deposited by CPCVD and PPCVD were prepared and their surface morphologies weremeasured by atomic force microscopy (AFM) (Fig. 3). In sample A, SiO_x with a flat surface was deposited by supplying a continuous RF power at a pressure of 11 Pa. In sample B, SiO_x with a large surface area was deposited by supplying a pulsed RF power at a pressure of 30 Pa. As illustrated in Fig. 3, PPCVD was able to increase the roughness ratio of SiO_x from 1.002 to 1.301.

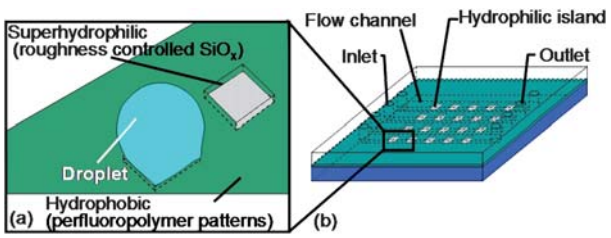

Fig. 1 Hydrophilic and hydrophobic combination for mTAS applications: (a) construction of hydrophilic islands and (b) integration image of hydrophilic islands for microfluidic applications.

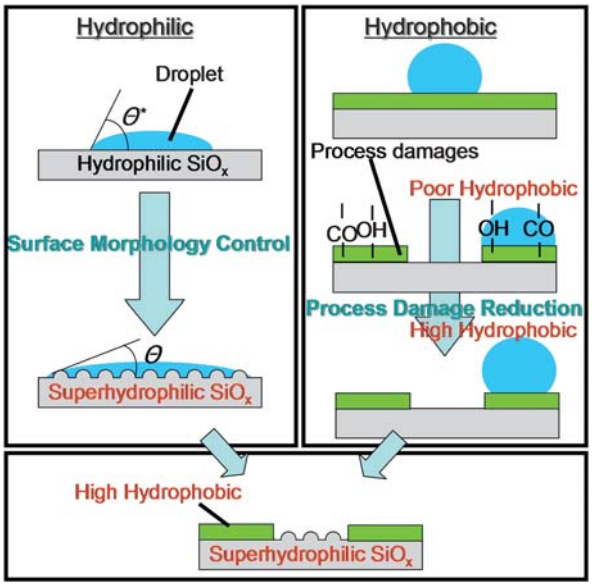

Fig. 2 The strategy for enhancement of wettability difference.

Combination of roughness-controlled SiO_x and perfluoropolymer patterning technique

Next, contact angles of SiO_x and the patterned CYTOP® (CTL-809M, Asahi Glass Co., Ltd) were evaluated with different fabrication parameters. It was previously difficult to pattern perfluoropolymer without reducing the hydrophobicity. CYTOP® was employed as a hydrophobic material. Our group investigated the influence of etching mask materials on the denaturation of the surface of CYTOP®.[10] The denaturation is caused by the evaporation process. Cu was employed as an etching mask to reduce the decline in the hydrophobicity. The postannealing process following the removal of an etching mask can reduce unsaturated bonds, and the process can restore the hydrophobic property at the surface of CYTOP®. The contact angle of the patterned CYTOP® was increased from 80.2° to 109.3° by using Cu as an etching mask and adding the postannealing process.

The fabrication process of the hydrophilic/hydrophobic patterned surface, as illustrated in Fig. 4, is described as follows:

(1) Deposition of SiO_x by PPCVD method

(2) Spin-coating and curing of CYTOP®

(3) Evaporation and patterning of metal (copper) as an O_2 plasma etching mask

(4) O_2 plasma etching of CYTOP®

(5) Removal of the etching mask, postannealing of CYTOP® at 230 °C

The contact angles of SiO_x samples are shown in Fig. 5. According to the experimental results shown in Fig. 5, sample B exhibited drastically improved hydrophilicity in each condition by increasing the surface area of SiO_x.

Table 1 The process parameters of CPCVD and PPCVD

Sample	Deposition method	RF supply/W	Total pressure/Pa	Gas
A	CPCVD	Continuously supply, power: 200	11	$Si(CH_3)_4$, O_2, Ar: continuously supply
B	PPCVD	Pulsed supply, RF duty: 10%, mean power: 200	30	$Si(CH_3)_4$: pulsed supply (duty 10%) O_2, Ar: continuously supply

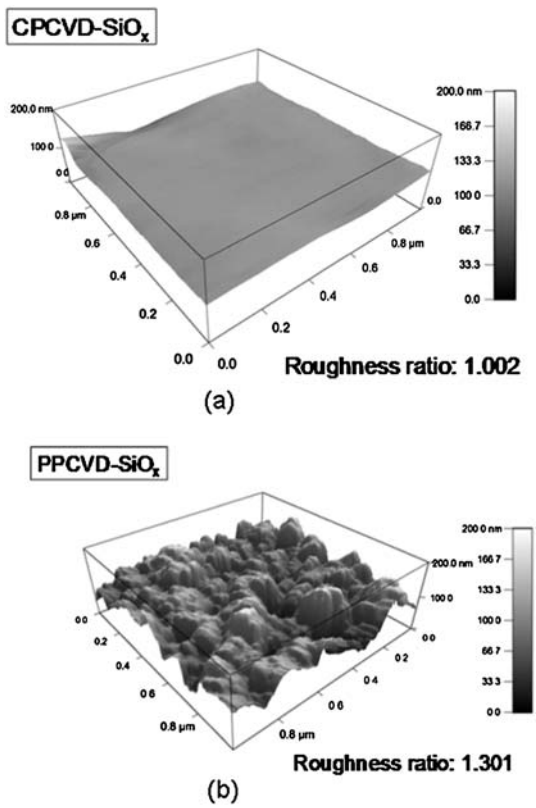

Fig. 3 Surface morphology of the deposited silicon oxide: (a) AFM image of sample A, deposited by continuous plasma CVD, and (b) AFM image of sample B, deposited by pulsed plasma CVD.

Because it is expected that the hydrophilicity is reduced by thermal load, the influence of the 230 °C postannealing in the patterning process for CYTOP® on the hydrophilicity of SiO_x is evaluated.

The postannealed sample B exhibited a successful reduction in contact angle from 55.6° to 22.7° compared with sample A, as shown in Fig. 5. Consequently, the combination of the patterned CYTOP® and sample B successfully enhanced the difference in contact angles from 54.3° to 86.6°.

Dome-shaped droplet generation utilizing one-side hydrophilic/hydrophobic functional surfaces

Droplet generation utilizing hydrophilic islands surrounded by hydrophobic regions in a microchannel was evaluated (Fig. 6). The shapes of generated droplets were evaluated when the wettability differences of the materials, flow rates, and surface tensions of liquids were changed. The wettability differences between the hydrophilic region and the hydrophobic region are

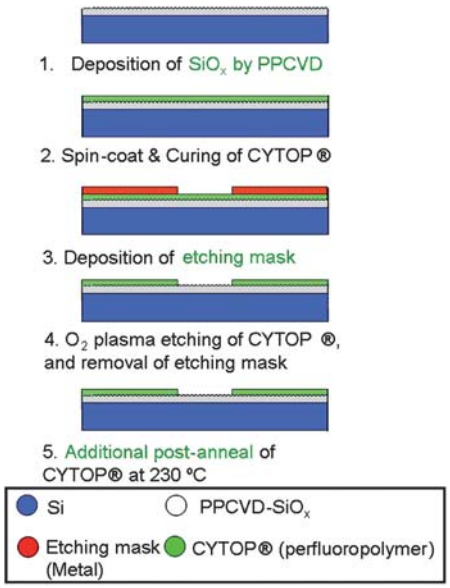

Fig. 4 Fabrication process of hydrophilic/hydrophobic functional surface.

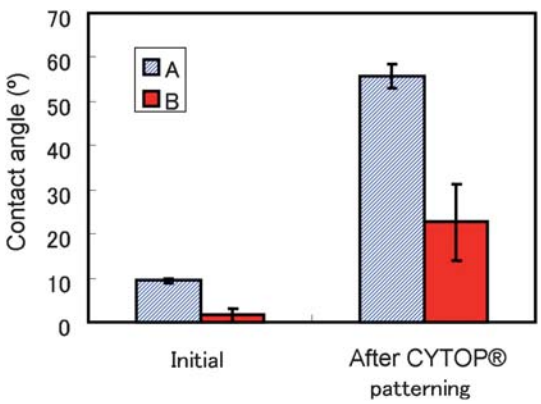

Fig. 5 Water contact angles on samples A and B (SiO_x deposited by CPCVD and PPCVD). Values are expressed as averages ± SD ($n = 3$).

listed in Table 2. The wettability differences of samples C and D are 54.3° and 86.6°, respectively. The structure of the flow channel with hydrophilic/hydrophobic patterns is shown in Fig. 6(a). The procedure of droplet generation is shown in Fig. 6(b). The test chip consisted of a hydrophilic/hydrophobic patterned substrate (CYTOP®/SiO_x/Si), a polydimethylsiloxane (PDMS) spacer, and a PDMS roof. Channel width and channel height were set at 1 mm and 0.5 mm, respectively.

Photographs of generated droplets in each of the samples are shown in Fig. 6(c) and (d). The upper and lower panels of Fig. 6(c) show water droplets generated by samples C and D,

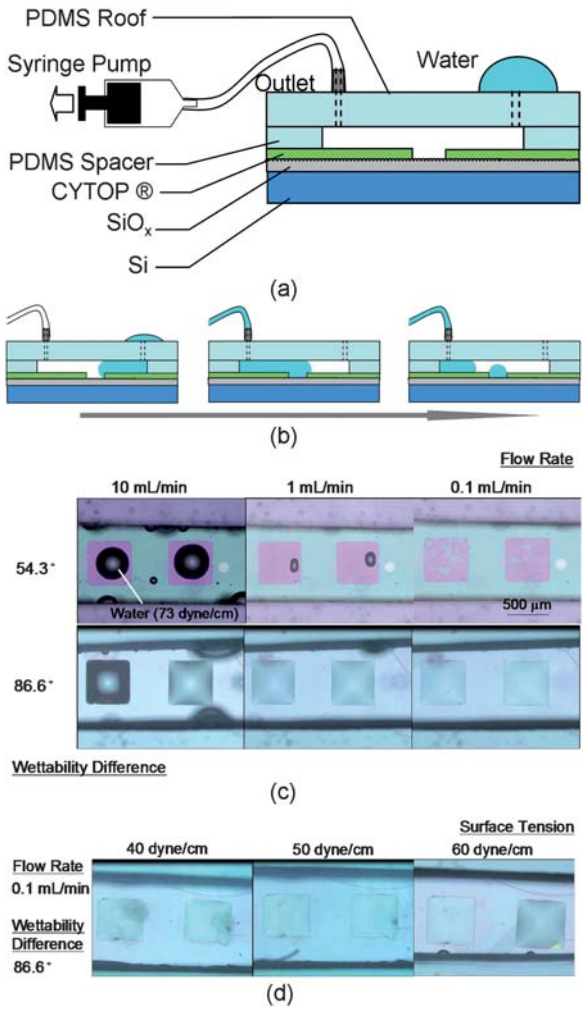

Fig. 6 Dome-shaped droplet generation test and results: (a) the structure of the flow channel integrated with hydrophilic/hydrophobic patterns, (b) procedure of droplet generation, and (c) water droplet generated at flow rates of 10, 1.0 and 0.1 mL min^{-1}, using samples C and D, and (d) reagent droplet generated at surface tensions of 40, 50 and 60 dyne cm^{-1}, using sample D, flow rates were set at 0.1 mL min^{-1}.

respectively. The surface tension of the water corresponded to 73 dyne cm^{-1}. The left, center, and right panels of Fig. 6(c) illustrate droplets generated at flow rates of 10, 1 and 0.1 mL min^{-1}, respectively.

It was difficult to split liquid into droplets at a low flow rate. Hydrophilic islands were filled with droplets almost completely in sample D (difference in contact angle was 86.6°), when liquid was vacuumed at a flow rate of 10 mL min^{-1} (Movie S1, ESI†). On the other hand, hydrophilic islands were partially filled with droplets in sample C (difference in contact angle was 54.3°) even at a flow rate of 10 mL min^{-1}. Thus, the combination of CYTOP® patterned by a Cu mask and SiO_x deposited by PPCVD is considered to be a promising component for droplet generation in microchannels. A larger wettability difference enabled the generation of droplets even at a flow rate of 0.1 mL min^{-1}, as shown in the lower-center and lower-right panels of Fig. 6(c).

Table 2 Materials and wettability difference of hydrophilic/hydrophobic patterns

Sample	Hydrophilic material	Hydrophobic material	Difference of contact angle/°
C	SiO_x (CPCVD, 11 Pa)	CYTOP®	54.3
D	SiO_x (PPCVD, 30 Pa)		86.6

Next, we evaluated droplet generation in low surface tension liquids as a preliminary study for blood metering. It has been reported that the surface tension of blood serum is around 50 dyne cm^{-1}.[13] Fig. 6(d) shows the droplets generated in the use of surface-tension-adjusted reagents at 40 dyne cm^{-1}, 50 dyne cm^{-1}, and 60 dyne cm^{-1} (wetting tension test mixture, Kanto Chemical Co., Inc.). The flow rate was set at 0.1 mL min^{-1}. Sample D could successfully split liquids into droplets when surface tensions were 40–73 dyne cm^{-1} (Movie S2, ESI†). Therefore, the developed hydrophilic/hydrophobic functional surface could be utilized to generate droplets from biological fluids.

Suspended-shape droplet generation utilizing both side hydrophilic/hydrophobic functional surfaces

We utilized hydrophilic islands formed on both the ceiling and the bottom in a flow channel for suspended-shape droplet generation. A suspended-shape droplet refers to a microsized liquid pillar in which the top and bottom are attached to the ceiling and the bottom of a flow channel. A schematic view of the suspended-shape droplet is shown in Fig. 7.

Optical detection and observation utilizing droplets in microfluidic devices has been reported to be one of the most promising applications of droplet manipulation technologies.[14,15] Observations of microbeads in dome-shaped droplets and suspended-shape droplets were performed. The averaged diameter of polystyrene microbeads is 15 mm. Fig. 8(a) shows a photograph of conventional dome-shaped droplet. Fig. 8(b) shows the magnified beads at the region A of Fig. 8(a). Since the shapes of beads were warped by refraction due to the surface curvature of the droplet, it was hard to observe beads existing in the surrounding region as shown in Fig. 8(a). It was suggested that the dome-shaped droplet was not suitable for observation of beads inside of the droplet. Fig. 8(c) and (d) show photographs of suspended-shape droplet and the magnified beads at the region B of Fig. 8(c), respectively. Beads in the suspended-shape droplet were clearly observed, as shown in Fig. 8(c) and (d). Furthermore, the

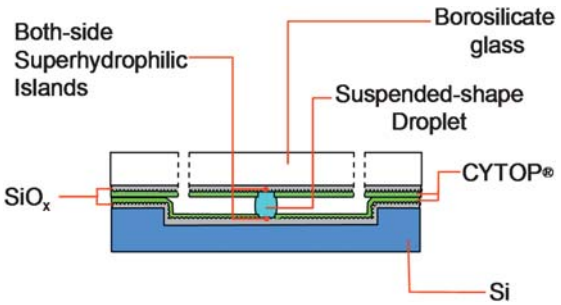

Fig. 7 Schematic view of the suspended-shape droplet.

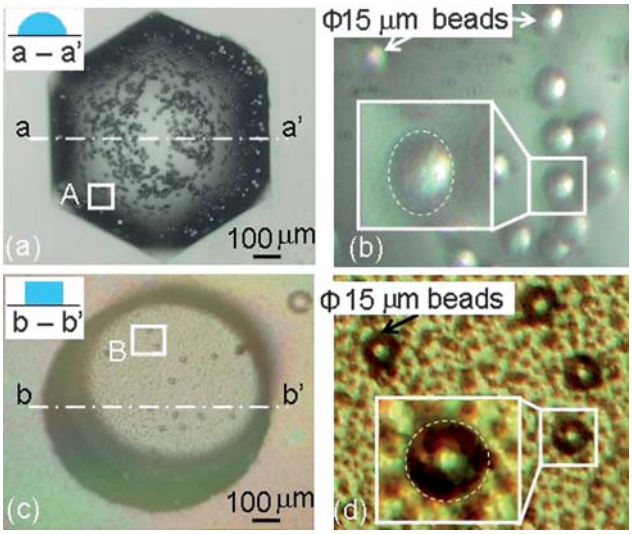

Fig. 8 Observed images of microbeads in the dome-shaped droplet and the suspended-shape droplet: (a and b) photographs of conventional dome-shaped droplet and the magnified beads at the region A of panel and (c and d) photographs of suspended-shape droplet and the magnified beads at the region B of panel.

suspended-shape droplet allowed observation of the whole projection area of the suspended-shape droplet because of uniform lighting.

Next, the effect of the flow rate on suspended-shape droplet generation was evaluated, as shown in Fig. 9. The flow channel was composed of grooved Si and borosilicate glass as a substrate and a roof plate, respectively. Superhydrophilic SiO_x was coated on the grooved Si plate and the borosilicate glass. CYTOP® layers were patterned on both SiO_x. The substrate and the roof plate were bonded to each other using the adhesion of the CYTOP® layer. The fluidic chip was bonded by applying 10 MPa at 120 °C. The channel height was 200 mm. Sample D in Table 2 was used as the combination of hydrophilic/hydrophobic

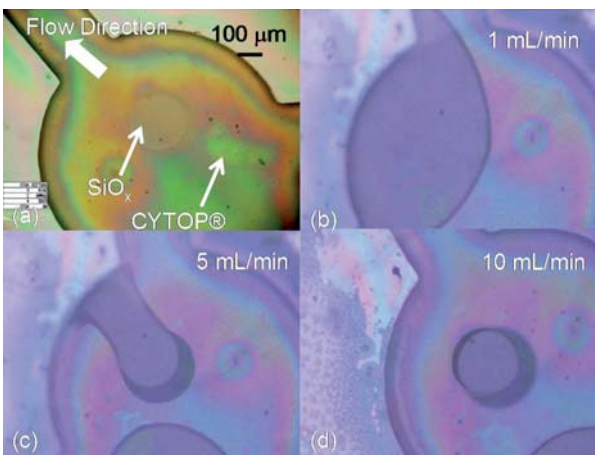

Fig. 9 Suspended-shape droplet generation test and results:(a) flow channel and hydrophilic/hydrophobic patterns, (b) residual liquid after water flowing at 1 mL min^{-1}, (c) residual liquid after water flowing at 5 mL min^{-1}, and (d) suspended-shape droplet after water flowing at 10 mL min^{-1}.

materials. A photograph of the fabricated device is shown in Fig. 9(a). Fig. 9(b)–(d) show water droplets generated at flow rates of 1, 5 and 10 mL min^{-1}, respectively.

The suspended-shape droplet was successfully generated when a flow rate of 10 mL min^{-1} was applied, as shown in Fig. 9(d) (Movie S3, ESI†). On the other hand, residual liquids were not split into droplets when liquids were vacuumed at flow rates of 1 and 5 mL min^{-1}, as shown in Fig. 9(b) and (c), respectively. The calculated volume of the generated droplet was 14.1 nL.

Handique *et al.* successfully split liquids into 0.5–125 nL of water droplets.[2,3] In our previous study, fluid at a flow rate of 1 mL min^{-1} was successfully split into 0.47–1.1 nL of water droplets.[4] However, both previous devices needed several valves for droplet generation and required two or three step operation. As compared with previous devices, the enhancement of wettability difference in the proposed device made it possible to form droplets by solely through hydrophilic/hydrophobic patterns in microchannels without complicated setup including valves.

Droplet transportation based on centrifugation

The titration process requires not only a droplet generation function but also a droplet handling function. Centrifugal force is often used as a driving force for on-chip liquid manipulation.[16–18] Droplet transportation utilizing centrifugation was also demonstrated as a preliminary test for on-chip titration.

The procedure of droplet transportation is shown in Fig. 10(a). Fig. 10(b)–(d) present photographs of droplets after centrifugal

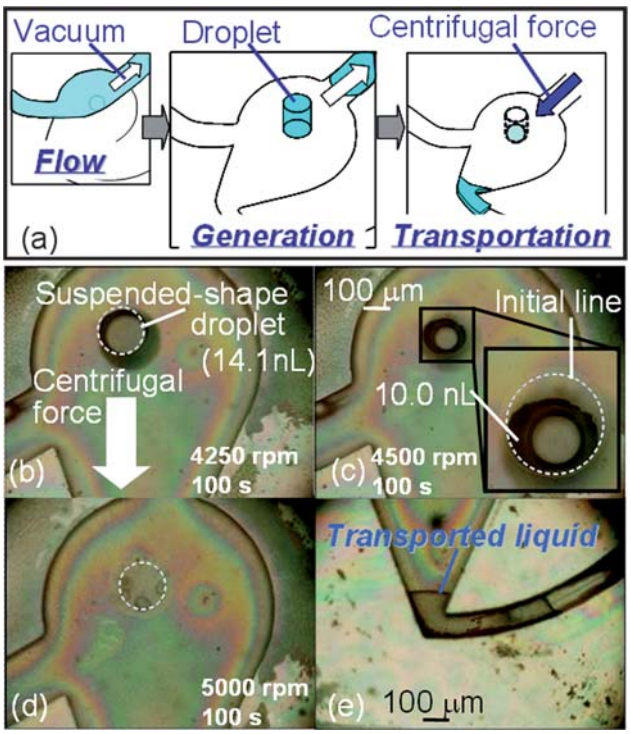

Fig. 10 Droplet manipulation by centrifugation: (a) procedure of droplet manipulation, (b–d) droplet after centrifugal spinning for 100 s, rotational speed of 4250 rpm (179.7 G), 4500 rpm (201.5 G), 5000 rpm (248.8 G), and (e) transported liquid at downstream of (d); channel height = 200 mm.

spinning for 100 s, the rotational speed was set at 4250, 4500, and 5000 rpm, respectively (centrifugal force = 179.7, 201.5 and 248.8 G, respectively). The 14.1 nL of suspended-shape droplet was generated before centrifugal transportation, as shown in Fig. 10(b). The distance between the generated droplet and the rotational axis was 8.9 mm. The faster the rotational speed applied, the larger the volume that was transported. The area of remaining droplets decreased as compared to the initial droplet shape, as shown in Fig. 10(c). When centrifugal force was applied, the remaining droplets tilted and then ejected from the rotational center to the outer side. The droplets were completely eliminated by increasing the rotational speed to 5000 rpm, as shown in Fig. 10(d). A photograph of the transported liquid downstream is shown in Fig. 10(e). The proposed droplet transportation mechanism can easily be combined with our previous reported cell/plasma centrifugation device.[19]

Conclusions

In this paper, a combination of roughness-controlled SiO_x realized by PPCVD and perfluoropolymer patterns is proposed. Droplet generation based on hydrophilic/hydrophobic patterns was demonstrated in microchannels. This paper revealed the following:

- SiO_x deposited by PPCVD at 30 Pa exhibited a particularly low contact angle at 22.7° even *via* 230 °C postannealing.
- The novel combination of hydrophilic PPCVD-SiO_x and hydrophobic CYTOP® was able to increase the difference in the contact angle from 54.3° to 86.6°.
- Droplet generation in the use of low surface tension reagents (such as 40 dyne cm^{-1} and 50 dyne cm^{-1}) was successful.
- Suspended-shape droplets were also successfully generated utilizing both side hydrophilic islands.
- Floating beads inside suspended-shape droplets could be clearly observed.
- Droplet transportation by centrifugal force was also successful.

Because the developed hydrophilic/hydrophobic combination enables the formation of droplets with desirable shape in microchannels, it can be considered a promising component in lab-on-a-chip applications. Future work will involve the application of the developed functional surface for droplet manipulation to biological liquid samples and reagents.

Acknowledgements

This research was supported by the Ritsumeikan Global Innovation Research Organization (R-GIRO) project in Ritsumeikan University.

References

1 S.-H. Lee, C.-S. Lee, B.-G. Kim and Y.-K. Kim, *J. Micromech. Microeng.*, 2003, **13**, 89–97.
2 K. Handique, D. T. Burke, C. H. Mastrangelo and M. A. Burns, *Anal. Chem.*, 2000, **72**(17), 4100–4109.
3 K. Handique, D. T. Burke, C. H. Mastrangelo and M. A. Burns, *Anal. Chem.*, 2001, **73**(8), 1831–1838.
4 T. Kobayashi and S. Konishi, Micro Electro Mech. Syst., 2010, *Proc. IEEE*, 2010, 1099–1102.
5 X. Wu and G. Shi, *Nanotechnology*, 2005, **16**, 2056–2060.
6 L. Zhai, M. C. Berg, F. C. Cebeci, Y. Kim, J. M. Milwid, M. F. Rubner and R. E. Cohen, *Nano Lett.*, 2006, **6**(6), 1213–1217.
7 T. Onda, S. Shibuichi, N. Satoh and K. Tsujii, *Langmuir*, 1996, **12**(9), 2125–2127.
8 Y. Lai, C. Lin, H. Wang, J. Huang, H. Zhuang and L. Sun, *Electrochem. Commun.*, 2008, **10**, 387–391.
9 Y. kaizuma, *J. Vac. Soc. Jpn.*, 2007, **50**(10), 635–638.
10 T. Kobayashi and S. Konishi, *IEEJ Transactions on Sensors and Micromachines*, 2009, **129**(7), 205–209.
11 B. Kakade, R. Mehta, A. Durge, S. Kulkarni and V. Pillai, *Nano Lett.*, 2008, **8**(9), 2693–2696.
12 C. Dorrer and J. Rühe, *Adv. Mater.*, 2008, **20**, 159–163.
13 A. Kratochvíl and E. Hrncír, *Gen. Physiol. Biophys.*, 2002, **21**, 47–53.
14 S.-Y. The, R. Lin, L.-H. Hung and A. P. Lee, *Lab Chip*, 2008, **8**, 198–220.
15 J. A. Schwartz, J. V. Vykoukal and P. R. C. Gascoyne, *Lab Chip*, 2004, **4**, 11–17.
16 D. Mark, T. Metz, S. Haeberle, S. Lutz, J. Ducree, R. Zengerle and F. Stetten, *Lab Chip*, 2009, **9**, 3599–3603.
17 S. Haeberle, T. Brenner, R. Zengerle and J. Ducree, *Lab Chip*, 2006, **6**, 776–781.
18 A. Oki, H. Ogawa, M. Nagai, S. Shinbashi, M. Takai, A. Yokogawa and Y. Horiike, *Mater. Sci. Eng., C*, 2004, **24**, 837–843.
19 T. Kobayashi, T. Funamoto, M. Hosaka and S. Konishi, *Jpn. J. Appl. Phys.*, 2010, **49**(7), 077001.

